

Regularized Super-Resolution for Diffusion MRI

S. Nedjati-Gilani¹, G. J. Parker², and D. C. Alexander¹

¹Centre for Medical Image Computing, University College London, London, United Kingdom, ²Imaging Science and Biomedical Imaging, University of Manchester, Manchester, United Kingdom

Introduction We present a new regularized super-resolution method, which finds fibre orientations and volume fractions on a sub-voxel scale and helps distinguish various fibre configurations such as fanning, bending and partial volume effects. We treat the task as a general inverse problem, which we solve by regularization and optimization, and run our method on human brain data.

Method For a set of image voxels l_i , $i=1\dots L$, and wavenumbers \mathbf{q}_k , $k=1\dots M$, we have measurements $A(l_i, \mathbf{q}_k)$. From these measurements, we want to find $\mathbf{p}(s_h)$, a set of model parameters in each of a set of super-resolution voxels s_h , where $h=1\dots H$. The forward problem is to estimate the measurements $A(l_i, \mathbf{q}_k)$ from $\mathbf{p}(s_h)$. Measurement estimates on the high-resolution grid come directly from the model parameters $\mathbf{p}(s_h)$, and we can estimate the measurements at l_i by $\tilde{A}(l_i, \mathbf{q}_k) = \sum_{h=1}^H \mu_{hi} A(s_h, \mathbf{q}_k)$, where μ_{hi} is a weighting coefficient that accounts for partial overlap between l_i and s_h , and could also account for factors such as the point-spread function and the slice profile. The inverse problem finds the model parameters from $A(l_i, \mathbf{q}_k)$. We solve the

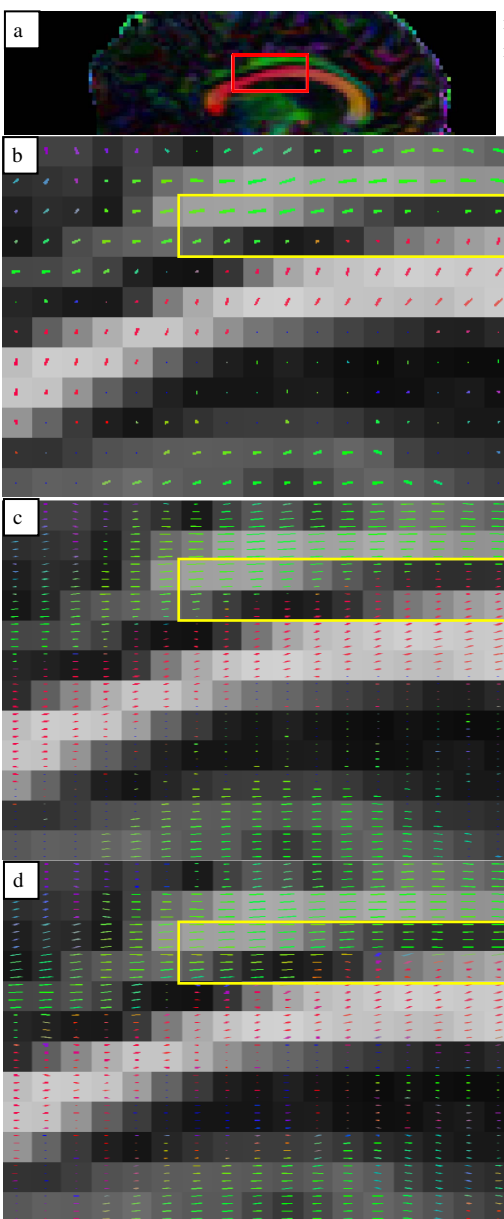


Figure 2: (a) FA map with the ROI highlighted, (b) initial fibre population estimates at the original spatial resolution, (c) fibre population reconstruction with linear interpolation and (d) reconstruction with regularized super-resolution.

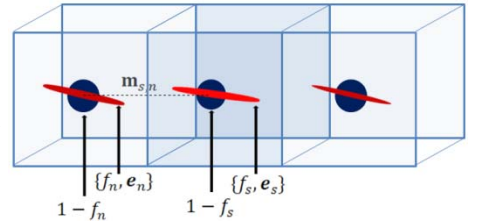


Figure 1 Illustration of a sub-voxel s with two voxels of its 6-neighbourhood, and associated fibre populations.

inverse problem with an optimization procedure to minimize an error metric between the observed and estimated measurements, subject to a spatial coherence constraint. For image I , we minimize the objective function $J(I) = \alpha T(I) + E(I)$, where $T(I)$ is a smoothing term ensuring that transitions of fibre populations of neighbouring sub-voxels are smooth, α is a weighting coefficient, and $E(I)$ is the error component defined as $E(I) = \sum_{i=1}^L \sum_{k=1}^M (A(l_i, \mathbf{q}_k) - \tilde{A}(l_i, \mathbf{q}_k))^2$. We use Behrens' model [1] with one fibre population so that $A(s, \mathbf{q}_k) = (1-f) \exp(-t|\mathbf{q}_k|^2 d) + f \exp(-td(\mathbf{e} \cdot \mathbf{q}_k)^2)$, where f is the volume fraction, \mathbf{e} is the orientation of the fibre population, d is the diffusivity and t is the diffusion time. The model parameter set for sub-voxel s_h is $\mathbf{p}(s_h) = \{d, f, \mathbf{e}\}$. We fit the model to the data [2] to find initial values $\mathbf{p}(l)$ for each large voxel l , and use nearest neighbour interpolation for initial values $\mathbf{p}(s)$ for each sub-voxel s . The subsequent optimizations use iterative voxel by voxel Levenberg-Marquardt least-squares minimization. For each sub-voxel s , we use the smoothing function $T(s) = \sum_{n \in N(s)} (f_n - f_s)^2 + (1 - |\mathbf{e}_n \cdot \mathbf{e}_s|)^2$, where $N(s)$ is the 6-neighbourhood of s . Figure 1 shows a sub-voxel with neighbouring voxels, and the terms used in $T(s)$. The first term in the smoothing function captures similarity of volume fraction of s with those of its neighbours, and the second term captures similarity of the fibre orientation of s with those of its neighbours. The smoothing function rewards similarities between fibre populations in s and its neighbours, and is minimized when $\mathbf{p}(n) = \mathbf{p}(s)$ for $\forall n \in N(s)$.

Experiments and Results We use our method on diffusion-weighted human brain data from a $128 \times 128 \times 32$ image with 61 diffusion-weighted images with a b -value of 1200 s mm^{-2} and one measurement at $\mathbf{q}=\mathbf{0}$, with eight repeats of each measurement, acquired in a Philips 3T Achieva scanner. For our experiment, we consider a region of interest of $12 \times 18 \times 14$ voxels in size, which includes part of the corpus callosum and the cingulum bundle, illustrated in Figure 2. We use our super-resolution method to quarter the slice thickness, thereby quadrupling the spatial resolution. We reconstruct the fibre populations at this higher resolution. We compare the results of our super-resolution method with those obtained using linear interpolation, shown in Figure 2. In the region highlighted in yellow, two distinct fibre populations are present in the corpus callosum (left-right, red) and in the cingulum (front-to-back, green). At the original resolution (b), partial volume effects artificially reduce the strength of the anisotropic component. The length of the lines are proportional to f . Linear interpolation (c) does not help in the partial volume region, and simply interpolates the low f . However, the super-resolution (d) correctly retains strong orientations by separating the two directional components and identifies the boundary between the two structures with sub-voxel accuracy.

Conclusions We can use our method to recover fibre configurations such as bending, fanning, and partial volume effects. Note that the method is very similar to fitting Behrens' model with multiple fibre orientations as in [3], but allows additional spatial separation of distinct directions. Future work includes considering alternative smoothing functions and using multiple fibre models for each sub-voxel to distinguish more complex fibre configurations such as genuine crossings from partial volume effects.

References: 1. T.E.J. Behrens *et al*, MRM 2003;50:1077-1088. 2. S. Nedjati-Gilani *et al*, ISMRM 2006;3169 3. T.E.J. Behrens *et al*, NeuroImage 2007;34(1):144-155.

Acknowledgements: This research was conducted with the aid of funding by Philips Medical Systems and EPSRC.